Fitoterapia 136 (2019) 104147

Contents lists available at ScienceDirect

Fitoterapia

journal homepage: www.elsevier.com/locate/fitote

C-Methylated flavanones from *the rhizomes of Matteuccia intermedia* and their α-glucosidase inhibitory activity

Xue Li[a], Ling-Juan Zhu[a], Jin-Peng Chen[a], Chen-Yu Shi[a], Li-Ting Niu[a], Xue Zhang[a,*], Xin-Sheng Yao[a,b,*]

[a] School of Traditional Chinese Materia Medica, Key Laboratory of Structure-Based Drug Design & Discovery, Ministry of Education, Shenyang Pharmaceutical University, Shenyang 110016, China
[b] Institute of Traditional Chinese Medicine & Natural Products, College of Pharmacy, Jinan University, Guangzhou 510632, China

ARTICLE INFO

Keywords:
Matteuccia intermedia
C-methylated flavanones
α-glycosidase inhibitory activity

ABSTRACT

One new flavanonol, demethylmatteucinol (**1**), and nine new flavanone glucoside derivatives, matteflavosides H-J (**2–4**) and matteuinterates A-F (**5–10**), were isolated from the rhizomes of *Matteuccia intermedia* C.Chr., along with 21 known flavanones (**11 − 31**). Notably, all of them contain *C*-methylation in the A-ring. The structures of the compounds were elucidated by spectroscopic methods and chemical derivatization. The *α*-glycosidase inhibition assay indicated that compounds **12–17** showed potent inhibitory activity with IC_{50} values of 12.4–69.7 μM, which suggested their hypoglycemic effect.

1. Introduction

The genus *Matteuccia* (Onocleaceae) includes about 5 species inhabitated mostly in north temperate regions. In China, there are 3 species named as *Matteuccia struthiopteris*, *M. orientalis* and *M. intermedia* [1]. A series of flavonoids, isocoumarins, phthalides, lignans, and stilbenes have been previously identified from the genus *Matteuccia*, in which flavanones with *C*-methylation at C-6 and/or C-8 are the main members [2–8]. The methyl groups of the *C*-methylated flavanone is derived from a chain extension with methylmalonyl-CoA in the second and third condensation of the biosynthetic reaction sequence [9]. Up to now, *C*-methylated flavanones and their glycosides with ***2′***-oxygenated, ***4′***-oxygenated, ***2′,4′***-dioxygenated, ***2′,5′***-dioxygenated, ***3′,4′***-dioxygenated, ***2′,3′,4′***-trioxygenated patterns in B ring have been reported from the genus *Matteuccia* [2,3,6,7]. Several *C*-methylated flavanones glycosides were further derivatized with a characteristic HMG group at C-3, C-4, or C-6 of the sugar moiety [2,3,6]. These diverse structures have resulted in wide range of pharmacological activities. In our former study on *M. struthiopteris*, a *C*-methylated flavanone as a potential antiviral agent against influenza A (H1N1) was obtained [7]. And a number of *C*-methylated flavanones from *M. orientalis* were reported to possess hypoglycemic activity in streptozotocin (STZ)-induced diabetic rats and anti-influenza virus (H1N1) effect [2,3,6]. Farrerol, a typical *C*-methylated flavanone, has been isolated from *M. orientalis*. Accumulating evidence suggested that farrerol exerts multiple biological activities, including antibechic [10], anti-inflammatory [11], antibacterial [12] and antioxidant activities [13], and a potential to treat and prevent cardiovascular diseases [14]. Desmethoxymatteucinol, obtained from *M. orientalis*, was found to exhibit moderate anti-inflammatory and cytotoxic activities [15]. In the course of our continual research for bioactive constituents from *Matteuccia* genus, one new flavanonol, demethylmatteucinol (**1**), and nine new flavanone glucoside derivatives, matteflavosides H-J (**2–4**) and matteuinterates A-F (**5–10**), along with 21 known ***C***-methylated flavanones (**11–31**) were isolated from the 60% EtOH extract of the *rhizomes* of *M. intermedia*. The structural elucidation of the new compounds and *α*-glucosidase inhibitory activity of **1–9**, **11–31** are described herein.

2. Experimental

2.1. General experimental

UV spectra were recorded by a UV-2201 UV-VIS recording spectrophotometer (Shimadzu, Kyoto, Japan). IR spectra were acquired on a Bruker IFS-55 spectrometer (Bruker, Rheinstetten, Germany) *with KBr disks.* Optical rotations were measured with an Anton Paar MCP 200 polarimeter (l = 1 cm) (Anton Paar GMBH, Graz, Austria). CD spectra were given by MOS 450 spectrometer (Bio-Logic Science, Grenoble,

* Corresponding authors at: School of Traditional Chinese Materia Medica, Key Laboratory of Structure-Based Drug Design & Discovery, Ministry of Education, Shenyang Pharmaceutical University, Shenyang 110016, China.
E-mail addresses: syzxalice@163.com (X. Zhang), tyaoxs@jnu.edu.cn (X.-S. Yao).

https://doi.org/10.1016/j.fitote.2019.04.002
Received 9 March 2019; Received in revised form 12 April 2019; Accepted 13 April 2019
Available online 22 April 2019
0367-326X/

France). NMR spectra were recorded using an AVANCE-600 NMR spectrometers (Bruker, Rheinstetten, Germany). HRESIMS were measured on a Waters Synapt G2 QTOF spectrometer (Waters, Milford, Massachusetts, USA). The analytical High Performance Liquid Chromatography (HPLC) was collected on an Agilent 1200 (Agilent Technologies, Santa Clara, California, USA) equipped with a DAD detector and a reversed-phase (RP) C18 column (5 μm, 4.60 × 250 mm; Phenomenex Luna, CA, USA). Semipreparative HPLC was performed applying a Shimadzu LC-6 CE with a UV SPD-20A detector, using a RP-C18 column (5 μm, 10 × 250 mm; Phenomenex Luna, CA, USA). Macroporous resin (Diaion HP20, Mitsubishi Chemical Corporation, Tokyo, Japan), silica gel (200–300 mesh, Qingdao Haiyang Chemical, Qingdao, China), ODS (60–80 μm, YMC, Tokyo, Japan), and Sephadex LH-20 (GE Healthcare Biosciences AB, Uppsala, Sweden) were used for column chromatography (CC).

2.2. Plant materials

The rhizomes of *M. intermedia* were collected from Hongyuan County, Aba Tibetan and Qiang Autonomous Prefecture (Sichuan, China) in November 2013, which were identified by Prof. Hao Zhang (West China School of Pharmacy, Sichuan University, China). A voucher specimen (YLXMI-2013) was deposited at the School of Traditional Chinese Materia Medica, Shenyang Pharmaceutical University, China.

2.3. Extraction and isolation

The dried rhizomes of *M. intermedia* (4.2 kg) were extracted with 60% EtOH (2 × 42 L, 2 h each). The dried extract (619.7 g) was suspended in H_2O (3 L) and subjected to a Diaion HP20 macroporous adsorptive resins column by gradient elution with EtOH/H_2O (0:100 to 95:5). The 50% EtOH eluate (36.5 g) was then separated over a silica gel column with a gradient system of CH_2Cl_2/MeOH (100:0 to 0:100) to afford 8 fractions (Fr. C1-C8). Fr. C5 was subjected to a Sephadex LH-20 column (CH_2Cl_2/MeOH, 1:1), followed by an ODS column eluted with MeOH/H_2O. The eluate of 40% MeOH was further purified by preparative HPLC (p-HPLC) (MeOH-0.1% formic acid, 50:50, monitored at 280 nm) to afford **8** (7.6 mg, t_R 28.8 min). Fr. C6 was divided into 7 fractions (Fr. C61-C67) by an ODS column with a system of MeOH/H_2O (30:70 to 100:0). Fr. C62 (eluted with 40% MeOH) and Fr. C65 (eluted with 50% MeOH) were applied to a Sephadex LH-20 column (CH_2Cl_2/MeOH, 1:1) followed by p-HPLC (MeOH-0.1% formic acid, 45:55 and 50:50, respectively, monitored with RID) to afford **10** (2.2 mg, t_R 30.5 min) and **9** (2.8 mg, t_R 40.1 min), respectively.

The 95% EtOH eluate (100.8 g) was loaded on a silica gel column eluted with CH_2Cl_2/MeOH (100:0 to 0:100) to afford 11 fractions (Fr. D1-D11). Compound **11** (120.0 mg) was crystallized in MeOH from Fr. D1. Fr. D3 was fractionated by an ODS column eluted with MeOH/H_2O (30:70 to 100:0) to afford 8 fractions (D31-D38). Fr. D34 (eluted with 60% MeOH) was further separated into **6** subfractions (D341–346) with CH_2Cl_2/MeOH (100:0 to 0:100). Purification of subfraction D341 by p-HPLC (55% MeOH, monitored at 280 nm) gave **14** (5.0 mg, t_R 63.7 min). Subfractions D342 and D343 were subjected to p-HPLC (62% MeOH, monitored at 220 nm) to yield **1** (5.0 mg, t_R 22.0 min), **12** (25.0 mg, t_R 25.0 min), **15** (284.3 mg, t_R 31.8 min), and **13** (58.8 mg, t_R 40.3 min), **16** (12.8 mg, t_R 26.3 min), **18** (10.0 mg, t_R 45.0 min), respectively. Fr. D6 and Fr. D8 were passed over a Sephadex LH-20 column eluted with CH_2Cl_2/MeOH (1:1), and a successive ODS column eluted with MeOH/H_2O, respectively. The 60% MeOH eluate of Fr. D6 and 40% MeOH eluate of Fr. D8 were purified by p-HPLC to yield **17** (11.3 mg, t_R 16.5 min) (55% MeOH, monitored at 220 nm) and **23** (4.5 mg, t_R 13.7 min) (MeCN-0.1% formic acid, 60:40, monitored at 280 nm), respectively. Fr. D9 was run on an ODS column with a gradient of MeOH/H_2O (20:80 to 100:0) to afford 10 fractions (D91-D910). Compounds **7** (6.4 mg, t_R 44.3 min) and **27** (105.8 mg, t_R 40.5 min) were afforded from the eluent of 40% MeOH (Fr. D94) purified by silica gel CC and p-HPLC (MeOH-0.1% formic acid, 45:55, monitored at 280 nm). Fr. D95 (eluted with 50% MeOH) was further separated into 9 subfractions (D951–959) using silica gel CC eluted with CH_2Cl_2/MeOH/H_2O (93:7:0 to 0:100:0). Subfractions D952 and D955 were subjected to p-HPLC (MeOH-0.1% formic acid, 50:50, monitored at 280 nm and monitored with RID, respectively) to yield **19** (1.1 mg, t_R 62.5 min) and **21** (1.1 mg, t_R 67.5 min), and **4** (2.1 mg, t_R 21.5 min) and **24** (5.4 mg, t_R 74.5 min), respectively. Purification of subfraction D957 by p-HPLC (MeOH-0.1% formic acid, 45:55, monitored at 220 nm) gave **25** (30.0 mg, t_R 80.0 min), **28** (8.8 mg, t_R 85.5 min) and **29** (5.9 mg, t_R 90.0 min). Fr. D96 (eluted with 50% MeOH) was purified by silica gel CC and p-HPLC (MeOH-0.1% formic acid, 55:45, monitored at 280 nm) to obtain **3** (7.2 mg, t_R 35.0 min) and **22** (11.2 mg, t_R 28.8 min). Compound **26** (63.0 mg) was crystallized in MeOH from Fr. D98 (eluted with 60% MeOH). Fr. D10 was subjected to an ODS column eluted with a gradient of MeOH/H_2O. The 40% MeOH eluate was loaded on a Sephadex LH-20 column, eluted with CH_2Cl_2/MeOH (1:1), and purified by p-HPLC (MeOH-0.1% formic acid, 45:55, monitored at 280 nm) to give **6** (11.2 mg, t_R 25.0 min), **20** (9.2 mg, t_R 22.1 min), **5** (8.2 mg, t_R 28.8 min), **2** (6.2 mg, t_R 40.4 min). Purification of the 50% MeOH eluate by Sephadex LH-20 CC and p-HPLC (MeOH-0.1% formic acid, 45:55, monitored at 220 nm) to obtain **30** (22.7 mg, t_R 103.8 min) and **31** (23.2 mg, t_R 105.0 min).

2.3.1. Demethylmatteucinol (1)

Light yellow amorphous powder; $[\alpha]_D^{20}$ −8.0 (*c* 0.05, MeOH); UV (MeOH) λ_{max} (log ε) 294 (3.93) nm; CD (*c* 1.58 × 10^{-3} M, MeOH) λ_{max} ($\triangle\varepsilon$) 217 (+19.21), 239 (+9.04), 257 (+4.98), 293 (−26.27), 330 (+3.31) nm; IR (KBr) ν_{max} 3408, 2925, 2853, 1630, 1515, 1462, 1422, 1384, 1250, 1179, 1114, 1030, 833 cm^{-1}; ^1H and ^{13}C NMR data, see Table 1; HRESIMS *m/z* 317.1023 $[M + H]^+$ (calcd. for $C_{17}H_{17}O_6$, 317.1025).

2.3.2. Matteflavoside H (2)

Yellow amorphous powder; $[\alpha]_D^{20}$ −38.0 (*c* 0.05, MeOH); UV (MeOH) λ_{max} (log ε) 282 (3.99) nm; CD (*c* 1.02 × 10^{-3} M, MeOH) λ_{max} ($\triangle\varepsilon$) 213 (+12.35), 233 (−3.02), 250 (+0.36), 287 (−9.03), 356 (+1.91) nm; ^1H and ^{13}C NMR data, see Table 1; HRESIMS *m/z* 493.1705 $[M + H]^+$ (calcd. for $C_{24}H_{29}O_{11}$, 493.1705).

2.3.3. Matteflavoside I (3)

Yellow amorphous powder; $[\alpha]_D^{20}$ −28.0 (*c* 0.05, MeOH); UV (MeOH) λ_{max} (log ε) 285 (4.02) nm; CD (*c* 1.02 × 10^{-3} M, MeOH) λ_{max} ($\triangle\varepsilon$) 211 (+26.72), 219 (−25.01), 251 (+0.66), 291 (+13.36), 319 (+1.60) nm; IR (KBr) ν_{max} 3386, 2920, 2851, 1630, 1522, 1431, 1384, 1280, 1166, 1125, 1068, 1038, 896, 832 cm^{-1}; ^1H and ^{13}C NMR data, see Table 1; HRESIMS *m/z* 491.1549 $[M - H]^-$ (calcd. for $C_{24}H_{27}O_{11}$, 491.1553).

2.3.4. Matteflavoside J (4)

Yellow amorphous powder; $[\alpha]_D^{20}$ −54.0 (*c* 0.05, MeOH); UV (MeOH) λ_{max} (log ε) 283 (4.02) nm; CD (*c* 1.08 × 10^{-3} M, MeOH) λ_{max} ($\triangle\varepsilon$) 219 (+30.97), 235 (−1.93), 249 (+3.35), 277 (−18.75), 350 (+4.64) nm; ^1H and ^{13}C NMR data, see Table 1; HRESIMS *m/z* 463.1617 $[M + H]^+$ (calcd. for $C_{23}H_{27}O_{10}$, 463.1604).

2.3.5. Matteuinterate A (5)

Light yellow amorphous powder; $[\alpha]_D^{20}$ -32.0 (*c* 0.05, MeOH); UV (MeOH) λ_{max} (log ε) 282 (4.35) nm; CD (*c* 0.77 × 10^{-3} M, MeOH) λ_{max} ($\triangle\varepsilon$) 218 (+12.12), 235 (−3.17), 250 (+1.01), 289 (−15.97), 354 (+4.26) nm; IR (KBr) ν_{max} 3424, 2924, 1721, 1631, 1514, 1443, 1402, 1384, 1275, 1176, 1126, 1071, 1024, 889, 833 cm^{-1}; ^1H and ^{13}C NMR data, see Table 2; HRESIMS *m/z* 637.2126 $[M + H]^+$ (calcd. for $C_{30}H_{37}O_{15}$, 637.2132).

Table 1
^{1}H and ^{13}C NMR data of compounds **1–4** (^{1}H 600 MHz, ^{13}C 150 MHz).

No.	**1**[a]		**2**[b]		**3**[b]		**4**[b]	
	δ_C, type	δ_H, (*J* in Hz)	δ_C, type	δ_H, (*J* in Hz)	δ_C, type	δ_H, (*J* in Hz)	δ_C, type	δ_H, (*J* in Hz)
2	85.4 CH	5.03 d (11.3)	78.8 CH	5.52 dd (12.3, 3.0)	74.2 CH	5.65 dd (12.9, 2.9)	74.8 CH	5.76 dd (12.8, 3.0)
3	74.6 CH	4.54 d (11.3)	43.2 CH_2	3.30 m, 2.86 dd (17.0, 3.0)	42.0 CH_2	3.30 m, 2.75 dd (17.1, 2.9)	42.3 CH_2	3.28 m, 2.88 dd (17.0, 3.0)
4	199.5C		199.4C		199.4C		199.5C	
5	163.7C		158.7C		158.3C		158.8C	
6	97.5 CH	6.00 s	112.1C		111.6C		112.0C	
7	167.7C		162.3C		161.9C		162.3C	
8	105.7C		111.0C		110.5C		111.1C	
9	162.1C		158.1C		158.2C		158.5C	
10	102.6C		105.7C		105.2C		105.6C	
1′	131.7C		132.2C		117.9C		125.9C	
2′	131.0 CH	7.51 d (8.6)	114.8 CH	6.99 d (2.3)	156.3C		155.2C	
3′	115.7 CH	7.01 d (8.6)	147.4C		105.2 CH	6.48 m	116.4 CH	6.93 d (7.9)
4′	162.5C		148.7C		160.8C		130.2 CH	7.24 td (7.9, 1.5)
5′	115.7 CH	7.01 d (8.6)	113.0 CH	6.98 d (8.3)	101.8 CH	6.46 m	120.1 CH	6.92 t (7.9)
6′	131.0 CH	7.51 d (8.6)	118.3 CH	6.92 dd (8.3, 2.3)	128.4 CH	7.36 d (8.3)	127.6 CH	7.51 dd (7.9, 1.5)
6-CH_3			9.6 CH_3	2.12 s	9.2 CH_3	2.10 s	9.6 CH_3	2.14 s
8-CH_3	8.3 CH_3	1.93 s	10.2 CH_3	2.11 s	9.7 CH_3	2.06 s	10.2 CH_3	2.12 s
4′-OCH_3	56.6 CH_3	3.86 s	56.6 CH_3	3.81 s	55.5 CH_3	3.73 s		
5-OH				12.15 s		12.13 s		12.14 s
3′-OH				9.15 s				9.88 s
2′-OH						10.03 s		
1″			105.1 CH	4.62 d (7.7)	104.7 CH	4.61 d (7.8)	105.1 CH	4.64 d (7.4)
2″			75.0 CH	3.33 m	74.6 CH	3.29 m	75.0 CH	3.33 m
3″			77.3 CH	3.26 m	76.8 CH	3.23 m	77.3 CH	3.26 m
4″			70.8 CH	3.17 m	70.3 CH	3.14 m	70.8 CH	3.17 m
5″			77.9 CH	3.09 m	77.5 CH	3.06 m	77.9 CH	3.10 m
6″			62.0 CH_2	3.66 m, 3.45 m	61.5 CH_2	3.61 t (10.0), 3.42 m	62.0 CH_2	3.66 m, 3.46 m

[a] Data measured in CD_3OD.
[b] Data measured in DMSO-d_6.

2.3.6. Matteuinterate B (6)

Yellow amorphous powder; $[\alpha]_D^{20}$ −30.0 (*c* 0.05, MeOH); UV (MeOH) λ_{max} (log ε) 284 (4.26) nm; CD (*c* 0.83 × 10^{-3} M, MeOH) λ_{max} ($\triangle\varepsilon$) 219 (+23.11), 233 (−3.04), 251 (+1.74), 288 (−12.25), 353 (+3.14) nm; IR (KBr) ν_{max} 3361, 2923, 1728, 1633, 1519, 1444, 1381, 1347, 1278, 1193, 1170, 1124, 1088, 1055, 1005, 824 cm^{-1}; ^{1}H and ^{13}C NMR data, see Table 2; HRESIMS *m/z* 607.2035 $[M + H]^+$ (calcd. for $C_{29}H_{35}O_{14}$, 607.2027).

2.3.7. Matteuinterate C (7)

Yellow amorphous powder; $[\alpha]_D^{20}$ −38.0 (*c* 0.05, MeOH); UV (MeOH) λ_{max} (log ε) 287 (4.20) nm; CD (*c* 0.77 × 10^{-3} M, MeOH) λ_{max} ($\triangle\varepsilon$) 218 (+17.06), 232 (−11.41), 247 (−0.69), 281 (−19.82), 305 (+0.77), 319 (−1.85), 352 (+3.31) nm; IR (KBr) ν_{max} 3423, 2923, 1631, 1510, 1402, 1384, 1273, 1206, 1174, 1127, 1073, 1040, 832 cm^{-1}; ^{1}H and ^{13}C NMR data, see Table 2; HRESIMS *m/z* 635.1977 $[M - H]^-$ (calcd. for $C_{30}H_{35}O_{15}$, 635.1976).

2.3.8. Matteuinterate D (8)

Light yellow amorphous powder; $[\alpha]_D^{20}$ −75.0 (*c* 0.1, MeOH); UV (MeOH) λ_{max} (log ε) 281 (3.86), 360.0 (3.43) nm; CD (*c* 0.81 × 10^{-3} M, MeOH) λ_{max} ($\triangle\varepsilon$) 214 (+7.72), 228 (−0.65), 279 (+2.99), 321 (−1.17), 372 (+1.84) nm; ^{1}H and ^{13}C NMR data, see Table 3; HRESIMS *m/z* 621.2183 $[M + H]^+$ (calcd. for $C_{30}H_{37}O_{14}$, 621.2183).

2.3.9. Matteuinterate E (9)

Yellow amorphous powder; $[\alpha]_D^{20}$ −98.0 (*c* 0.1, MeOH); UV (MeOH) λ_{max} (log ε) 285 (4.03), 360.0 (3.48) nm; CD (*c* 0.77 × 10^{-3} M, MeOH) λ_{max} ($\triangle\varepsilon$) 218 (+13.26), 234 (−6.33), 250 (+2.08), 284 (−8.03), 303 (0.31), 320 (−1.88), 363 (+3.88) nm; IR (KBr) ν_{max} 3397, 2947, 1631, 1432, 1276, 1206, 1175, 1126, 1029, 832 cm^{-1}; ^{1}H and ^{13}C NMR data, see Table 3; HRESIMS *m/z* 651.2283 $[M + H]^+$ (calcd. for $C_{31}H_{39}O_{15}$, 651.2289).

2.3.10. Matteuinterate F (10)

Brown amorphous powder; [α] −108.0 (*c* 0.1, MeOH); UV (MeOH) λ_{max} (log ε) 282 (4.09), 359 (3.56) nm; CD (*c* 0.63 × 10^{-3} M, MeOH) λ_{max} ($\triangle\varepsilon$) 217 (+23.18), 288 (−19.77), 359 (+2.90) nm; IR (KBr) ν_{max} 3411, 2949, 2835, 1631, 1428, 1272, 1172, 1125, 1031, 1008, 881, 832 cm^{-1}; ^{1}H and ^{13}C NMR data, see Table 3; HRESIMS *m/z* 799.2668 $[M + H]^+$ (calcd. for $C_{36}H_{47}O_{20}$, 799.2661).

2.4. Biological assays

2.4.1. α-Glycosidase inhibition assay

The assay was conducted in 96-well microtiter plates referring to the procedures as previously described [16]. Briefly, test compounds (in DMSO) of different concentrations, the enzyme (0.5 U/mL, from *Saccharomyces cerevisiae*, Sigma, Germany), and *p*-nitrophenyl-α-D-glucopyranoside (*p*-NPG) (5.0 mM, Sigma, Switzerland) were dissolved by 67.0 mM sodium phosphate buffer (pH 6.8), respectively. Four kinds of wells were made. Test wells contained 112 μL of buffer, 20 μL of enzyme, and 8 μL of sample. Test blank wells contained 132 μL of buffer and 8 μL of sample. Negative control wells contained 112 μL of buffer, 20 μL of enzyme, and 8 μL of DMSO. Negative blank wells contained 132 μL of buffer and 8 μL of DMSO. The plates were preincubated for 5 min at 37 °C. Then the reaction was initiated by the addition of 20 μL of p-NPG and incubated for 30 min at 37 °C. The absorbance of released product (*p*-nitro phenol) by measured at 405 nm. The α-glucosidase inhibition rate (%) = [1- (OD_{test} - $OD_{test\ blank}$)/($OD_{negative\ blank}$ - OD_{blank})] × 100%. All tests were performed in triplicate, with acarbose used as a positive control.

2.4.2. Molecular docking

Molecular docking was performed to predict the binding mode between the α-glucosidase protein and flavanones in the Discovery Studio 3.5 software. The crystal structure of Gal1p (PDB Code: 2AJ4) was obtained from the Protein Data Bank [17] and then minimized using the

Table 2
^{1}H and ^{13}C NMR data of compounds **5–7** (^{1}H 600 MHz, ^{13}C 150 MHz, DMSO-d_6).

No.	**5**		**6**		**7**	
	δ_C, type	δ_H, (J in Hz)	δ_C, type	δ_H, (J in Hz)	δ_C, type	δ_H, (J in Hz)
2	79.0 CH	5.49 dd (12.4, 2.6)	79.0 CH	5.52 dd (12.7, 2.7)	74.7 CH	5.74 dd (13.0, 2.9)
3	43.5 CH_2	3.25 m, 2.83 dd (16.7, 2.6)	43.2 CH_2	3.32 m, 2.84 dd (17.3, 2.7)	42.2 CH_2	3.30 m, 2.86 dd (17.0, 2.9)
4	199.4C		199.5C		199.5C	
5	158.8C		158.8C		158.8C	
6	111.9C		112.0C		112.2C	
7	162.0C		162.0C		162.0C	
8	111.1C		111.0C		111.0C	
9	158.2C		158.3C		158.4C	
10	105.7C		105.8C		105.7C	
1′	132.3C		130.0C		126.6C	
2′	114.8 CH	7.05 brs	129.0 CH	7.37 d (8.7)	148.8C	
3′	147.8C		116.2 CH	6.85 d (8.7)	117.1 CH	6.85 m
4′	148.8C		158.6C		115.1 CH	6.84 m
5′	113.0 CH	6.96 d (8.3)	116.2 CH	6.85 d (8.7)	153.1C	
6′	118.1 CH	6.89 dd (8.3, 1.3)	129.0 CH	7.37 d (8.7)	113.2 CH	7.08 d (2.5)
6-CH_3	9.5 CH_3	2.09 s	9.5 CH_3	2.09 s	9.6 CH_3	2.14 s
8-CH_3	10.1 CH_3	2.06 s	10.1 CH_3	2.05 s	10.1 CH_3	2.13 s
4′-OCH_3	56.6 CH_3	3.81 s				
4′-OH				9.64 s		
5-OH		12.13 s		12.15 s		12.14 s
2′-OH						9.40 s
5′-OCH_3					56.3 CH_3	3.74 s
1″	104.9 CH	4.67 d (7.4)	104.9 CH	4.66 d (7.6)	104.6 CH	4.79 d (7.7)
2″	74.8 CH	3.35 m	74.8 CH	3.34 m	72.9 CH	3.52 m
3″	76.9 CH	3.30 m	76.9 CH	3.28 m	78.2 CH	4.90 t (9.9)
4″	70.8 CH	3.22 m	70.7 CH	3.24 m	68.6 CH	3.38 m
5″	74.5 CH	3.34 m	74.5 CH	3.35 m	77.5 CH	3.25 m
6″	64.0 CH_2	4.23 d (9.9), 4.07 m	63.9 CH_2	4.25 d (10.3), 4.07 m	61.6 CH_2	3.66 m, 3.48 m
1‴	171.2C		171.2C		171.0C	
2‴	46.8 CH_2	2.56 overlapped, 2.47 d (13.6)	46.5 CH_2	2.63 d (14.4), 2.49 d (14.4)	47.3 CH_2	2.72 d (13.6), 2.58 d (13.6)
3‴	69.8C		69.8C		70.2C	
4‴	46.8 CH_2	2.40 s	46.4 CH_2	2.44 m	46.3 CH_2	2.47 m
5‴	173.8C		173.5C		174.0C	
6‴	28.1 CH_3	1.19 s	28.1 CH_3	1.21 s	28.5 CH_3	1.33 s

CharMM27 force field and the MMFF94 charge with a distance-dependent dielectric and conjugate gradient method. The optimized structures were used for all subsequent calculations. The Libdock module embedded in Discovery Studio was used to dock the compounds to the binding site of α-glucosidase, which was defined by the location of AMPPNP. The default parameters were used in the docking process.

2.5. Acid hydrolysis and determination of the absolute configuration of the monosaccharides of compounds **2–10**

Glucosyl moiety identification in the structures was carried out according to the methods of literatures [18,19]. Compound (**2** − **10**) (1.0 mg each) was hydrolyzed with 2 M HCl for 2 h at 90 °C. After evaporating under vacuum, the residue was dissolved in H_2O and extracted with $CHCl_3$, then the aqueous layer was dried in vacuo. The residue of **2–4** was dissolved in distilled water (1.0 mL), and analyzed by LC-NetII/ADC HPLC with OR-4090 optical rotation detector equipped with a Shodex Asahipak NH2P-50 4E column (1.0 mL/min, CH_3CN-H_2O, 3:1, 20 μL), respectively. The sugar moiety was identified to be D-glucose by comparison of the retention time and orientation with those of authentic samples at (t_R 9.0 min, positive peak) [18]. The residue of **5–10** was dissolved in 0.5 mL pyridine containing L-cysteine methyl ester (3.0 mg, Sigma, USA) and heated at 60 °C for 1 h. Then, *o*-tolyl isothiocyanate (5 μL) (Alfa Aesar, U.K.) was added and directly analyzed by HPLC after heating for 1 h at 60 °C. Analytical HPLC was acquired on an RP-C18 column (5 μm, 4.60 × 250 mm; Phenomenex Luna) at 35 °C with isocratic elution (CH_3CN-0.1% formic acid, 25:75, 0.8 mL/min, monitored at 250 nm). The authentic glucoses, D-glucose and L-glucose (Sigma, USA), were subjected to the same process. The peaks of the standard D-glucose and L-glucose derivatives were recorded at t_R 20.9 (L-Glc) and 23.6 (D-Glc) min. The glucosidic derivatives of **5–10** were identified as D-glucose based on the t_R = 22.8 min [19].

2.6. Determination of the absolute configuration of HMG in compounds **5–8**, and **10**

To establish the absolute configuration of the HMG group, compounds **5–8** (5 mg each) and **10** (1.5 mg) were dissolved by 0.3 mL DMF containing (*S*)-1-phenylethylamine (Aladdin, USA) (2 equiv), Et_3N (Aladdin, USA) (3 equiv), PyBOP (Aladdin, USA) (1.5 equiv), and HOBt (Aladdin, USA) (2 equiv) under ice-cooling, respectively. The reaction was quenched with diluted HCl after stirring for 9 h at room temperature, and the residue was dried in vacuo. Amide **A** was obtained by separation of the residue using a Waters Sep-Pak®Vac normal-phase column (CH_2Cl_2/MeOH, 30:1, 20:1, 15:1 and 10:1) and was identified by LC-MS analysis. The THF (0.3 mL) solution containing amide A was added to $LiBH_4$ (15 equiv. of **A**) under ice cooling which was stirred for 24 h at 25 °C and quenched with dilute HCl. The resulting mixture was extracted with EtOAc and concentrated. Purification of the extract was achieved by a Waters Sep-Pak®Vac normal-phase column ($CHCl_3$/MeOH, 40:1, 30:1, 20:1 and 15:1) to furnish **B**. Then **B** was acetylated by Ac_2O (5 equiv. of A) in pyridine (30 μL) and stirred for 24 h at 25 °C. The reaction mixture was diluted with H_2O and extracted with EtOAc. Further purification of the product was conducted by analytical HPLC with 75% MeOH (monitored at 220 nm) under isocratic condition at 0.8 mL/min to obtain **C**. The ^{1}H NMR spectrum (Fig. S98, Supporting Information) of **C** was found to be consistent with that of (3*R*)-5-*O*-acetyl-1-[(*S*)-phenylethyl]mevalonamide upon comparison, rather than

Table 3
^{1}H and ^{13}C NMR data of compounds **8–10** (^{1}H 600 MHz, ^{13}C 150 MHz, DMSO-d_6).

No.	**8**		**9**		**10**	
	δ_C, type	δ_H, (*J* in Hz)	δ_C, type	δ_H, (*J* in Hz)	δ_C, type	δ_H, (*J* in Hz)
2	79.1 CH	5.52 dd (12.6, 3.2)	74.8 CH	5.72 dd (13.1, 2.7)	74.4 CH	5.93 dd (13.3, 2.6)
3	43.2 CH_2	3.34 m, 2.84 dd (17.0, 3.2)	42.3 CH_2	3.25 m, 2.87 dd (17.0, 2.7)	43.4 CH_2	3.11 dd (16.9, 13.3), 2.77 dd (16.9, 2.6)
4	199.6C		199.4C		199.6C	
5	158.9C		158.8C		158.8C	
6	112.0C		112.1C		112.1C	
7	162.0C		162.0C		162.0C	
8	111.0C		110.9C		111.0C	
9	158.3C		158.4C		158.6C	
10	105.8C		105.7C		105.8C	
1′	130.0C		126.6C		121.5C	
2′	129.0 CH	7.37 d (8.5)	148.8C		155.7C	
3′	116.1 CH	6.85 d (8.5)	117.0 CH	6.85 d (8.8)	102.8 CH	6.84 d (2.4)
4′	158.6C		115.1 CH	6.83 dd (8.8, 2.5)	161.1C	
5′	116.1 CH	6.85 d (8.5)	153.1C		108.6 CH	6.75 dd (8.7, 2.4)
6′	129.0 CH	7.37 d (8.5)	113.1 CH	7.08 d 2.5	127.7 CH	7.54 d (8.7)
6-CH_3	9.5 CH_3	2.08 s	9.6 CH_3	2.094 s	9.6 CH_3	2.10 s
8-CH_3	10.1 CH_3	2.05 s	10.0 CH_3	2.091 s	10.1 CH_3	2.09 s
4′-OCH_3			56.3 CH_3	3.73 s	56.1 CH_3	3.80 s
5-OH		12.15 s				12.18 s
1″	104.9 CH	4.65 d (7.5)	104.9 CH	4.68 d 7.7	104.9 CH	4.66 d (7.8)
2″	74.8 CH	3.35 m	74.7 CH	3.34 m	74.8 CH	3.35 m
3″	76.9 CH	3.29 m	76.9 CH	3.30 m	76.9 CH	3.30 m
4″	70.7 CH	3.22 m	70.7 CH	3.23 m	70.8 CH	3.22 m
5″	74.5 CH	3.33 m	74.5 CH	3.37 m	74.5 CH	3.38 m
6″	64.0 CH_2	4.26 dd (11.8, 2.0), 4.07 dd (11.8, 6.1)	64.0 CH_2	4.28 brd (10.5), 4.07 m	64.1 CH_2	4.26 brd (10.4), 4.06 dd (11.8, 6.4)
1‴	171.1C		171.1C		171.3C	
2‴	46.5 CH_2	2.64 d (14.0), 2.48 d (14.0)	46.6 CH_2	2.65 d (14.0), 2.49 d (14.0)	46.6 CH_2	2.59 d (14.0), 2.49 d (14.0)
3‴	69.9C		69.8C		69.8C	
4‴	46.0 CH_2	2.56 d (2.1)	46.0 CH_2	2.55 overlapped	46.8 CH_2	2.41 brs
5‴	171.8C		171.8C		174.4C	
6‴	28.2 CH_3	1.22 s	28.1 CH_3	1.21 s	28.2 CH_3	1.21 s
5‴-CH_3	52.0 CH_3	3.58 s	52.0 CH_3	3.58 s		
1⁗					102.6 CH	4.80 d (7.2)
2⁗					74.1 CH	3.26 m
3⁗					77.2 CH	3.28 m
4⁗					70.9 CH	3.16 m
5⁗					78.2 CH	3.40 m
6⁗					61.8 CH_2	3.78 m, 3.48 m

the (3*S*) isomer that was previously reported [2,20].

(3*R*)-5-*O*-Acetyl-1-[(*S*)-phenylethyl]-mevalonamide (**5C**): Colorless oil; ^{1}H NMR ($CDCl_3$, 600 MHz) δ_H 7.28–7.37 (5H, m, 1′-C_6H_5), 6.04 (1H, d, *J* = 6.0 Hz, NH), 5.15 (1H, quintet, *J* = 7.1 Hz, H-1′), 4.24 (2H, m, H-5), 2.41 and 2.29 (each 1H, d, *J* = 14.5 Hz, H-2), 2.05 (3H, s, 5-$OCOCH_3$), 1.86 (2H, m, H-4), 1.51 (3H, d, *J* = 7.1 Hz, H-2′), 1.24 (3H, s, 3-CH_3); ESIMS *m/z* 292.0 [M - H] $^-$.

3. Results and discussion

The 60% EtOH extract of the rhizomes of *M. intermedia* was partitioned by macroporous adsorptive resins eluted with EtOH/H_2O (0:100 to 95:5). The 95% EtOH eluate was subjected to chromatographic separation using silica gel, ODS, Sephadex LH-20, and semipreparative HPLC to yield 31***C***-methylated flavonoids. The presence of D-glucosyl in compounds **2–10** was determined by acid hydrolysis and HPLC analyses [18,19]. The configuration of the anomeric carbon was indicated to be β based on the large coupling constant of the anomeric proton (*J* = 6.0–8.0 Hz).

Compound **1** was obtained as a light yellow amorphous powder. Its molecular formula was deduced as $C_{17}H_{16}O_6$ by ^{13}C NMR data and HRESIMS, giving a quasimolecular ion peak $[M + H]^+$ at *m/z* 317.1023 (calcd 317.1025). The UV absorption band was at 294 nm, characteristic of a flavanonol. ^{1}H NMR spectrum displayed a pair of protons at δ_H 4.54 and 5.03 with *J* = 11.3 Hz, which suggested that **1** was a flavanonol derivative. Apart from these two proton signals, the ^{1}H NMR spectrum clearly showed an AA′XX′ coupling system at δ_H 7.01 (2H, d, *J* = 8.6 Hz, H-3′, 5′) and 7.51 (2H, d, *J* = 8.6 Hz, H-2′, 6′)] in B-ring, a singlet proton at δ_H 6.00 (1H, s, H-6) in A-ring, one methyl at δ_H 1.93 (3H, s, 8-CH_3) and one methoxy group at δ_H 3.86 (3H, s, 4′-OCH_3). The HMBC correlations for –CH_3 (δ_H 1.93)/C-7, C-8, C-9, and –OCH_3 (δ_H 3.86)/C-4′ revealed a methyl located at C-8 and a methoxy group located at C-4′ (Fig. 2). And the molecular formula of **1**, in combination with the ^{1}H and ^{13}C NMR data, indicated that three hydroxy groups should be located at C-3, C-5 and C-7, respectively. The circular dichroism (CD) spectrum of **1** showed negative Cotton effect at 293 nm and positive Cotton effect at 330 nm, suggesting the absolute configurations at C-2 and C-3 were *R*, *R* [21]. Based on the foregoing evidence, the structure of **1** was elucidated as (2*R*,3*R*)-3,5,7-trihydroxy-8-methyl-4′-methoxydihydroflavanol, named as demethylmatteucinol.

Compound **2** was isolated as a yellow amorphous powder with the molecular formula of $C_{24}H_{28}O_{11}$ on the basis of HRESIMS at *m/z* 491.1549 [M - H] $^-$. The UV spectrum was suggestive of a flavanone derivative with absorption band at 282 nm. The ^{1}H and ^{13}C NMR data of **2** were similar to those of **16**, except for an additional β-D-glucopyranosyl moiety. The HMBC correlation between the anomeric proton at δ_H 4.61 (H-1″) and C-7 indicated that the glycosidation of 7-OH in **2** (Fig. 2). The CD spectrum of **2** showed a negative Cotton effect at 287 nm, suggesting that the absolute configuration at C-2 was *S* [21]. Thus, compound **2** was elucidated as (2*S*)-3′-hydroxymatteucinol-7-*O*-β-D-glucopyranoside, named as matteflavoside H.

Compound **3** was obtained as a yellow amorphous powder. The

HRESIMS of **3** showed a quasimolecular ion peak [M - H] $^-$ at *m/z* 491.1549 (calcd 491.1553), supporting the same molecular formula of $C_{24}H_{28}O_{11}$ as **2**. Its ^{1}H and ^{13}C NMR data were similar to those of **2**, with the differences in data attributed to B-ring. The HMBC spectrum of **3** showed correlations of H-2/C-1′, C-2′, C-6′, H-5′/C-3′, C-4′, H-6/C-2′, C-4′, C-5′, and δ_H 3.73 (4′-OCH_3)/C-4′, revealing the locations of the methoxy group at C-4′, and the hydroxy group at C-2′ in **3** instead of at C-3′ in **2**. The CD spectrum of **3** showed a positive Cotton effect at 288 nm, suggesting that the absolute configuration at C-2 was *R* [21]. Therefore, the structure of **3** was elucidated as (2*R*)-2′-hydroxymatteucinol-7-*O*-*β*-D-glucopyranoside, named as matteflavoside I.

Compound **4** was isolated as a yellow amorphous powder. The ^{1}H and ^{13}C NMR spectra of **4** exhibited spectroscopic features similar to those of the known flavanone glucoside matteucin 7-*O*-*β*-D-glucoside [6]. Analyses of the 2D NMR suggested an identical planar structure to that of **4**, which was also supported by the molecular formula of $C_{23}H_{26}O_{10}$ determined by HRESIMS (*m/z* 463.1617 [M + H] $^+$, calcd for $C_{23}H_{27}O_{10}$, 463.1604). The CD spectrum showed a negative Cotton effect at 277 nm, being opposite to matteucin 7-*O*-*β*-D-glucoside, which indicated as *S* configuration at C-2 in **4** [21]. Therefore, compound **4** was identified as (2*S*)-matteucin 7-*O*-*β*-D-glucopyranoside, named as matteflavoside *J*.

Compound **5**, a light yellow amorphous powder, had a molecular formula of $C_{30}H_{36}O_{15}$ based on a quasi-molecular ion peak at *m/z* 637.2126 [M + H] $^+$ in HRESIMS. The UV spectrum revealed the presence of a flavanone skeleton with absorption band at 282 nm. Detailed analyses of the 1D NMR (Table 2) revealed that **5** was similar to **2**, and the key differences were the presence of two carbonyls, two methylenes, one oxygenated quaternary carbon, and one methyl. The HMBC correlations for H-2‴/C-1‴, H-4‴/C-5‴, and 3‴-CH_3/ C-2‴, C-3‴, C-4‴, in combination with the molecular formula, revealed the presence of a 3-hydroxy-3-methylglutaryl (HMG) fragment. The HMG substituent was placed at C-6″ of the glucosyl unit by HMBC correlations between H-6″ (δ_H 4.23 and 4.07) and C-1‴ (δ_C 171.2) (Fig. 2). The absolute configuration of the chiral carbon in the HMG group was determined with the literature method including amidation, reduction and acetylation to yield 5-*O*-acetyl-1-[(*S*)-phenylethyl]mevalonamide (Scheme 1). Its ^{1}H NMR data were identical to those of (3*R*)-5-*O*-acetyl-1-[(*S*)-phenylethyl]-mevalonamide rather than the (3*S*) isomer [20]. The CD spectrum of **5** showed a negative cotton effect at 289 nm, suggesting that the absolute configuration at C-2 was *S* [21]. Therefore, compound **5** was named as (2*S*)-3′-hydroxymatteucinol-7-*O*-[6″-*O*-((*S*)-3-hydroxy-3-methylglutaryl)]-*β*-D-glucopyranoside, named as matteuinterate A.

Compound **6** was obtained as a yellow amorphous powder. The HRESIMS ion at *m/z* 607.2035 [M + H] $^+$ established its molecular formula as $C_{29}H_{34}O_{14}$. On careful analyses of the 1D NMR data and molecular formula between **6** and **5**, the differences in **6** involved the absence of a methoxy group, and a 1,4-disubstituted B-ring replacing a 1,3,4-trisubstituted B-ring, which deduced the position of the hydroxy group was at C-4′ in **6**. The absolute configuration of the HMG group was also determined to be *S* using the method mentioned above. The CD spectrum of **6** showed a negative Cotton effect at 288 nm, suggesting that the absolute configuration at C-2 was *S* [21]. Thus, compound **6** was established as (2*S*)-farrerol-7-*O*-[6″-*O*-((*S*)-3-hydroxy-3-methylglutaryl)]-*β*-D-glucopyranoside, named as matteuinterate B.

Compound **7**, a yellow amorphous powder, had a molecular formula of $C_{30}H_{36}O_{15}$ based on its HRESIMS analysis (*m/z* 635.1977, [M - H] $^-$, calcd for 635.1976). The UV, ^{1}H NMR, and ^{13}C NMR data closely resembled those of the known flavanone glucoside matteuorienate *J* (**30**), which revealed that they possessed identical skeleton, but differed in the linkage position between the glucosyl moiety and the HMG fragment. The HMBC correlation of H-3″/C-1‴ indicated that the HMG fragment was attached to the C-3″ of the glucosyl moiety. The downfield shift of C-3″ from 76.7 in **30** to 78.2 in **7** further confirmed the above conclusion. The 3*S*-configuration of the HMG moiety was determined as described above. The CD spectrum of **7** showed a negative Cotton effect at 281 nm, suggesting that the absolute configuration at C-2 was *S* [21]. Therefore, the structure of **7** was defined as (2*S*)-methoxymatteucin-7-*O*-[3″-*O*-((*S*)-3-hydroxy-3-methylglutaryl)]-*β*-D-glucopyranoside, named as matteuinterate C.

Compound **8**, obtained as a light yellow amorphous powder, was assigned the molecular formula $C_{30}H_{36}O_{14}$ by HRESIMS data (*m/z* 621.2183, [M + H] $^+$, calcd for 621.2183). A detailed comparison of ^{1}H and ^{13}C NMR spectral data between **8** and **6** indicated that compound **8** was a methylated derivative of **6** based on an additional methoxy group at δ_H 3.58 (3H, s) and δ_C 52.0. The HMBC correlation between –OCH_3 (δ_H 3.58) and the carbonyl carbon at δ_C 171.8 confirmed the methylation of C-5‴ in the HMG unit. Experiment for determining the absolute configuration of the HMG moiety in **8** was attempted, but appropriate derivatives could not be obtained due to the methylation of C-5‴ in the HMG moiety. Due to the isolates with the HMG group from the genus *Matteuccia* both in our study and in the literature possessing *S*-configuration in the HMG unit [2], the asymmetric C-3‴ in compound **8** was proposed to be an *S*-configuration because of a shared biogenesis. In turn, the positive Cotton effect of **8** at 279 nm in the CD spectrum revealed the structure of **8** as 2*R* configuration [21]. Thus, compound **8** was assigned as (2*R*)-farrerol-7-*O*-[6″-*O*-((*S*)-3-hydroxy-3-methyl-methylglutaryl)]-*β*-D-glucopyranoside, named as matteuinterate D.

Compound **9** was obtained as a yellow amorphous powder. The molecular formula of $C_{31}H_{38}O_{15}$ was confirmed on the basis of HRESIMS data (*m/z* 651.2283, [M + H] $^+$, calcd for 651.2289). The ^{1}H and ^{13}C NMR data of **9** were similar to those of **7**, except for the presence of an extra methoxy group at δ_H 3.58 (3H, s) and δ_C 52.0. Compound **9** was a methylated derivative at C-5‴ of **7** confirmed by the HMBC correlation between –OCH_3 (δ_H 3.58) and C-5‴ in the HMG unit. The absolute configuration of C-3‴ in the HMG group was also

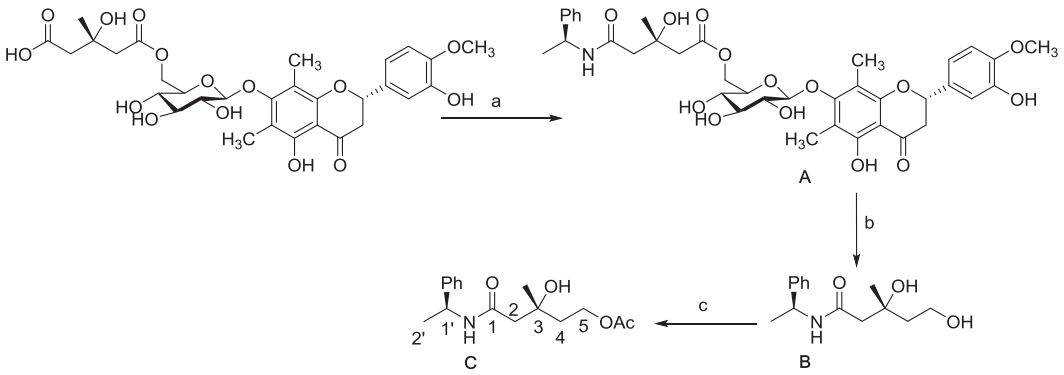

Scheme 1. Determination of the absolute configuration of HMG group in compound **5** (representive). Reagents and conditions: (a) (*S*)-1-phenylethylamine, PyBOP, HOBt, Et_3N, DMF; (b) $LiBH_4$, THF; (c) Ac_2O, pyridine [2,20].

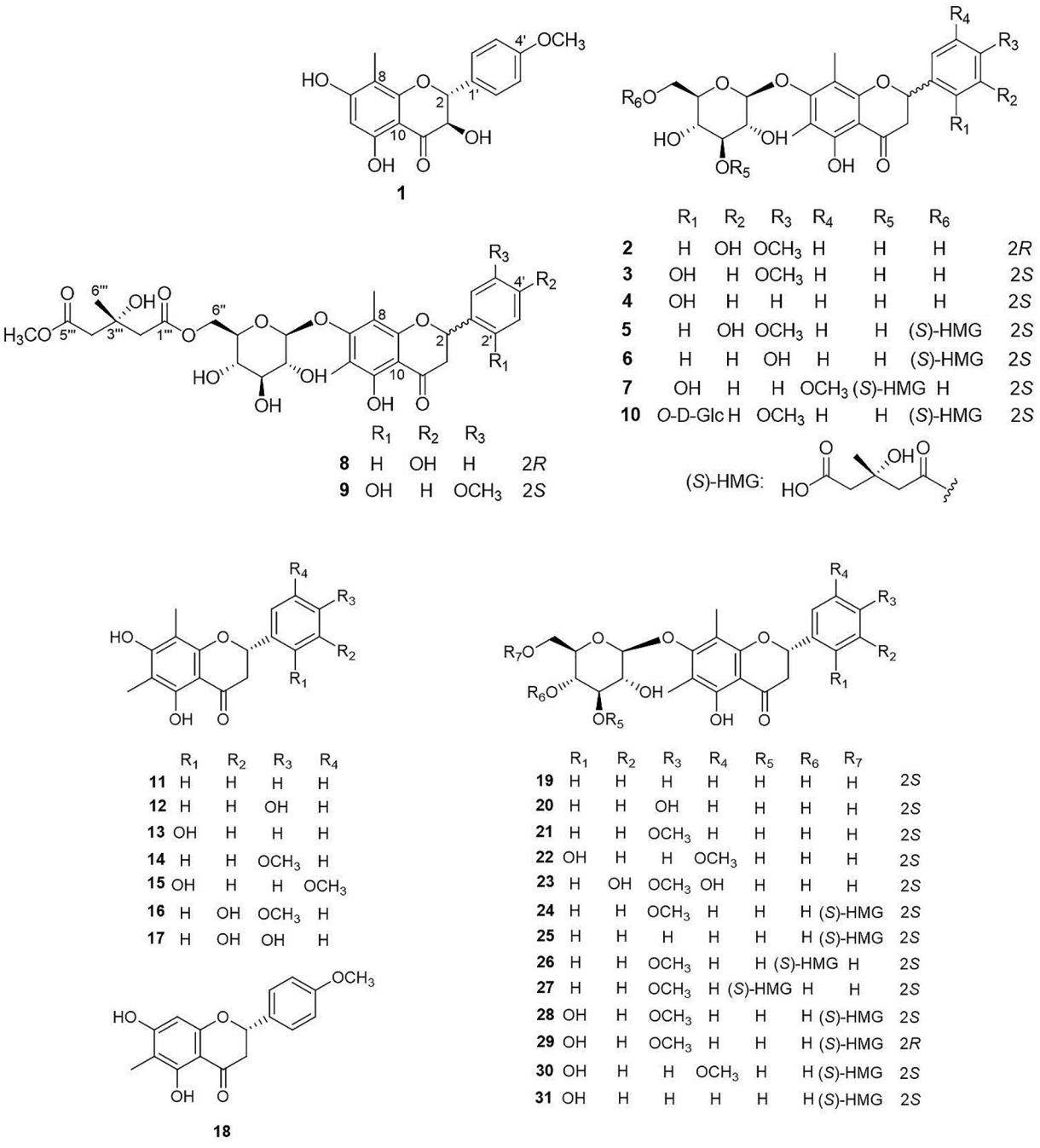

Fig. 1. Chemical structures of compounds **1–31** isolated from *Matteuccia intermedia*.

proposed to be *S* because of a shared biogenesis. The negative Cotton effect at 283 nm implied a 2*S* absolute configuration [21]. Thus, **9** was determined as (2*S*)-methoxymatteucin-7-*O*-[6″-*O*-((*S*)-3-hydroxy-3-methyl-methylglutaryl)]-*β*-D-glucopyranoside, named as matteuinterate E.

Compound **10** was obtained as a brown amorphous powder, with a molecular formula of $C_{36}H_{46}O_{20}$ by HRESIMS (*m/z* 799.2668 [M + H]$^+$, calcd for 799.2661). The ^{1}H and ^{13}C NMR data were similar to those of **28**, except for an additional *β*-D-glucosyl unit. The extra D-glucose moiety was linked to the aglycone at C-2′, which was indicated by the HMBC correlation of H-1‴/C-2′ (Fig. 2). The CD spectrum of **10** showed a negative Cotton effect at 288 nm, suggesting that the absolute configuration at C-2 was *S* [21]. Further determination of the absolute configuration of the HMG group as described above confirmed the structure of **10** to be (2*S*)-2′-hydroxymatteucinol-7-*O*-[3″-*O*-((*S*)-3-hydroxy-3-methylglutaryl)]-*β*-D-glucopyranoside-2′-*O*-*β*-D-glucopyranoside, named as matteuinterate F.

Twenty-one known structures were identified as demethoxymateucinol (**11**) [22], farrerol (**12**) [23], matteucin (**13**) [24], matteucinol (**14**) [25], methoxymatteucin (**15**) [25], 3′-hydroxy-matteucinol (**16**) [26], cyrtominetin (**17**) [27], 5,7-dihydroxy-4′-methoxy-6-methyl-flavanone (**18**) [28], demethoxymateucinol 7-*O*-glucoside (**19**) [2], farrerol 7-*O*-glucoside (**20**) [29], matteucinol 7-*O*-glucoside (**21**) [2], myrclacitrin II (**22**) [2], matteflavoside G (**23**) [7], matteuorienate A (**24**) [3], matteuorienate B (**25**) [3], matteuorienate D (**26**) [2], matteuorienate F (**27**) [2], matteuorienate H (**28**) [2], matteuorienate I (**29**) [2], matteuorienate J (**30**) [2] and matteuorienate K (**31**) [2] (Fig. 1) by comparing their chemical and spectroscopic characteristics with the reported data. Among the isolated *C*-methylated flavanones with substituted B ring, the 2′-hydroxyl, 4′-hydroxyl, 3′,4′-dihydroxyl and 3′,5′-dihydroxyl substituted derivatives were found. Compounds 12

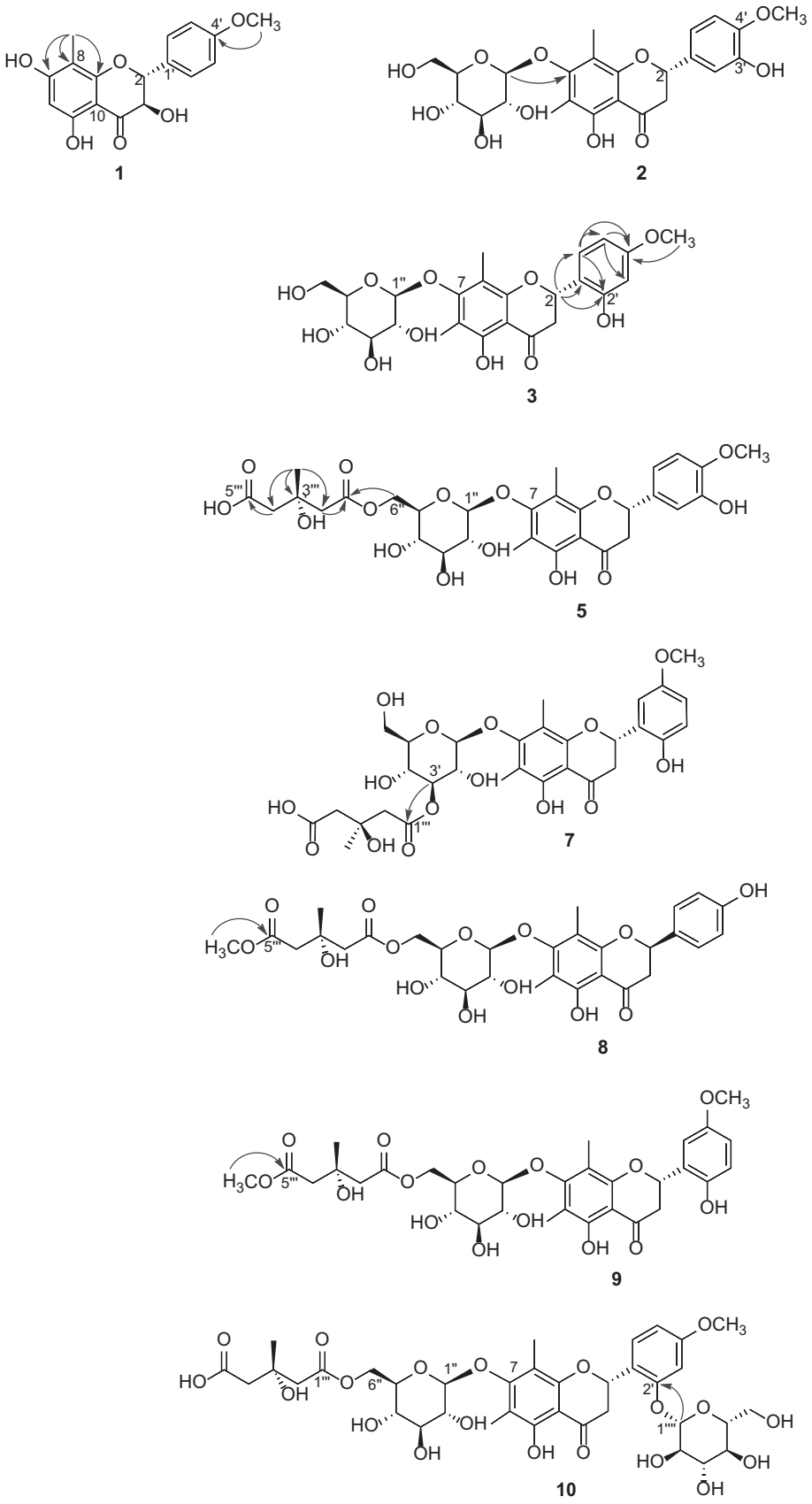

Fig. 2. Selected key HMBC (→) correlations of **1–3**, **5**, **7–10**.

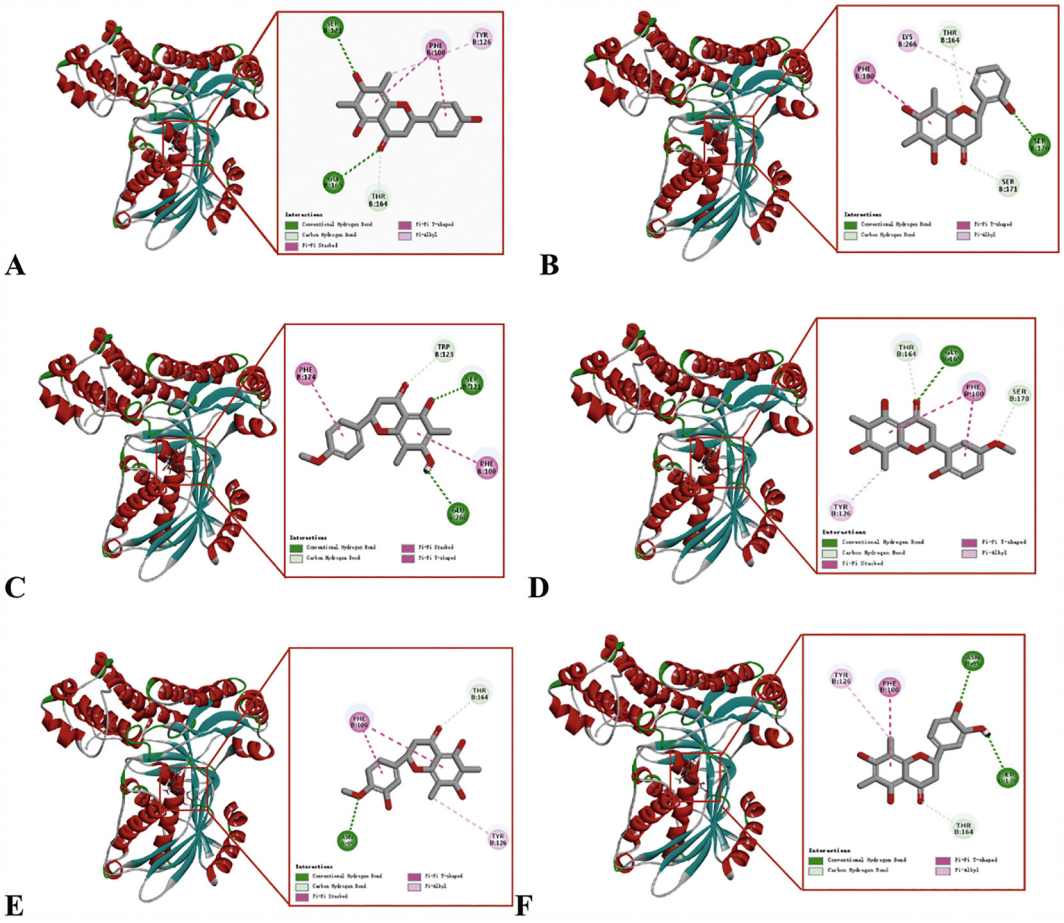

Fig. 3. The binding modes of compounds **12–17** with the key residues on α-glucosidase. (A) compound **12**. (B) compound **13**. (C) compound **14**. (D) compound **15**. (E) compound **16**. (F) compound **17**.

and 14 were converted into compounds **17 and 16** by flavonoid 3′-hydroxylase (F3′H), respectively [30]. And previous reports suggested that the B ring appeared to undergo stepwise oxidation from 2′-hydroxyl to 2′,4′-dioxygenated derivatives, as represented by compound **13** to **15** [31].

α-Glucosidase is the most important enzyme in carbohydrate digestion in vivo. Inhibition of α-glucosidase can lead to prevent excess glucose absorption at the small intestine, which controls the blood glucose level and is considered an effective way to prevent diabetes and obesity exacerbation [32]. The hypoglycemic activity in vitro of all isolates except for **10** (due to limited amount of sample available) was evaluated via an α-glucosidase inhibitory assay. Acarbose, a common α-glycosidase inhibitor, was used as a positive control and showed IC_{50} value of 172.3 μM. Compounds **12–17** showed potent inhibitory activity (IC_{50} values of 12.4–69.7 μM) (Table 4), revealing their hypoglycemic effect. In our study, all the active flavanones in the α-glucosidase inhibitory assay possessed 7-OH, and all the 7-*O*-glycoside derivatives were inactive. These results suggested that the hydroxy group at C-7 of flavanones should be crucial for the potent inhibitory activity on α-glucosidase, which was consistent with previous report [33]. The decreasing inhibitory effect after glycosylation may be caused by increasing molecular size and polarity, and resulting the increase of the steric hindrance, which weakens the binding interaction between flavanones and α-glucosidase. Compounds **12–17**, possessing 6- and 8-methyl in A-ring and hydroxy or methoxy group in B-ring, showed stronger activity than other aglycones (**1**, **11**, **18**). Therefore, the hydroxylation or methoxylation in the B-ring of flavanones and the simultaneous methylation at C-6 and C-8 may contribute to the inhibitory activity. Compound **17**, with two hydroxy groups in Bring, displayed the strongest α-glucosidase inhibitory activity. Compounds **15** and **16** with both hydroxy and methoxy groups in the B-ring were less active than **17**. For compounds **12–14** possessing mono oxygenated B ring, compound **14** with a methoxy group showed higher inhibitory activity than compounds **12 and 13** with a hydroxy group. Based on the above results, it is reasonable to hypothesize that the methylation of solitary hydroxy group in B-ring is favourable to increase the binding stability of compounds and α-glycosidase, and further enhance the inhibitory

Table 4
α-Glucosidase inhibitory activity of compounds **1–9**, **11–31**.

Compound	IC_{50} (μM)[a]	Compound	IC_{50} (μM)[a]
1	> 200	**18**	> 200
2	> 200	**19**	> 200
3	> 200	**20**	> 200
4	> 200	**21**	> 200
5	> 200	**22**	> 200
6	> 200	**23**	> 200
7	> 200	**24**	> 200
8	> 200	**25**	> 200
9	> 200	**26**	> 200
11	> 200	**27**	> 200
12	44.1 ± 0.42	**28**	> 200
13	37.6 ± 2.67	**29**	> 200
14	28.0 ± 3.56	**30**	> 200
15	69.7 ± 7.86	**31**	> 200
16	43.6 ± 3.96	Acarbose	172.3 ± 14.7
17	12.4 ± 2.66		

[a] IC_{50} values represent the means ± standard deviation (SD) of three parallel measurements.

capacity. On the contrary, the methylation of hydroxy group in the disubstituted B ring significantly increased the steric hindrance, especially at C-5′ position in the 2,5-disubstituted pattern, which was in accordance with the result of **15**.

To further reveal the potential binding mode of α-glucosidase and the candidate compounds, molecular docking was performed using Discovery Studio 3.5 software package. The 3′,4′-phenolic hydroxy groups of B-ring in compound **17** formed two vital hydrogen bonds with the side chains of Asn-95 and Ser-170 located in the bottom of binding pocket. In addition, a Pi-Pi stacking interaction was observed between the aromatic A-ring of **17** and the side chain of Phe-100. The 5,7-phenolic hydroxy groups of A-ring oriented towards solvent polarizable surface, which further stabilized the complex (Fig. 3). The above interactions suggested that compound **17** could bind with α-glucosidase with a reasonable conformation. Then the aromatic A and/or B-ring of compounds **12–17** shared common Pi-Pi stacking interactions with Phe-100, and compound **14** was discovered an extra Pi-Pi stacking interaction between the B-ring and Phe-174. There are two H-bond interactions between the 7-hydroxyl and Ser-121, and the carbonyl and Gly-165 in **12**; two H-bond interactions between 5-hydroxyl and Ser-121, and 7-hydroxyl and Glu-268 in **14**. There is one H-bond interaction between the 2′-hydroxyl of **13** and Ser-170, the carbonyl of **15** and Gly-165, the methoxy group of **16** and Asn-95, respectively. These results show compounds **12–17** could form stable interactive conformation with the binding site of α-glucosidase, and Pi-Pi stacking interaction of A- and B-ring as well as the H-bond interaction of the substituted hydroxy groups are vital to stability of the complex. The results further support the inhibitory activity obtained by the α-glucosidase assay and structure-activity relationship rules.

Conflict of interest

The authors declared that they have no conflicts of interest to this work.

Acknowledgements

The authors thank Prof. Hao Zhang, at Sichuan University, China for the botanical identification. We also thank Institute of Traditional Chinese Medicine & Natural Products, College of Pharmacy, Jinan University for the HRESIMS measurement.

Appendix A. Supplementary data

Supplementary data to this article can be found online at https://doi.org/10.1016/j.fitote.2019.04.002.

References

[1] Flora of China Editorial Committee, Chinese Academy of Sciences, vol. 4, Science Press, 1999, p. 164.
[2] J. Huh, T. Ha, K.B. Kang, K.H. Kim, W.K. Oh, J. Kim, S.H. Sung, *C*-Methylated flavonoid glycosides from *pentarhizidium orientale* rhizomes and their inhibitory effects on the H1N1 influenza virus, J. Nat. Prod. 80 (2017) 2818–2824.
[3] S. Kadota, P. Basnet, K. Hase, T. Namba, Matteuorienate A and B, two new and potent aldose reductase inhibitors from *Matteuccia orientalis* (Hook.) Trev, Chem. Pharm. Bull. 42 (1994) 1712–1714.
[4] P. Shao, X. Zhang, B. Li, W.H. Jiao, L.J. Wu, X.S. Yao, New isocourmarin and phthalide derivatives from the rhizomes of *Matteuccia orientalis*, Chem. Pharm. Bull. 58 (2010) 1650–1654.
[5] L.J. Zhu, Y. Song, P. Shao, X. Zhang, X.S. Yao, Matteucens I-J, phenolics from the rhizomes of *Matteuccia orientalis*, J. Asian Nat. Prod. Res. 20 (2017) 62–66.
[6] P. Basnet, S. Kadota, K. Hase, T. Namba, Five new *C*-methyl flavonoids, the potent aldose reductase inhibitors from *Matteuccia orientalis* Trev, Chem. Pharm. Bull. 43 (1995) 1558–1564.
[7] B. Li, Y. Ni, L.J. Zhu, F.B. Wu, F. Yan, X. Zhang, X.S. Yao, Flavonoids from *Matteuccia struthiopteris* and their anti-influenza virus (H1N1) activity, J. Nat. Prod. 78 (2015) 987–995.
[8] L.J. Zhu, F. Yan, J.P. Chen, N. Zhang, X. Zhang, X.S. Yao, 8-O-4′ Neolignan glycosides from the aerial parts of *Matteuccia struthiopteris*, Chin. Chem. Lett. 27 (2016) 63–65.
[9] J. Schroder, S. Raiber, T. Berger, A. Schmidt, J. Schmidt, A.M. Soares-Sello, E. Bardshiri, D. Strack, T.J. Simpson, M. Veit, G. Schroder, Plant polyketide synthases: a chalcone synthase-type enzyme which performs a condensation reaction with methylmalonyl-CoA in the biosynthesis of C-methylated chalcones, Biochemistry 37 (1998) 8417–8425.
[10] J. Zhu, D. Li, J. Jin, L. Wu, Binding analysis of farrerol to lysozyme by spectroscopic methods, Spectrochim. Acta A Mol. Biomol. Spectrosc. 68 (2007) 354–359.
[11] C.P. Chung, J.B. Park, K.H. Bae, Pharmacological effects of methanolic extract from the root of Scutellaria baicalensis and its flavonoids on human gingival fibroblast, Planta Med. 61 (1995) 150–153.
[12] Y. Cao, Q. Chu, J. Ye, Chromatographic and electrophoretic methods for pharmaceutically active compounds in *Rhododendron dauricum*, J. Chromatogr. B. Analyt. Technol. Biomed. Life Sci. 812 (2004) 231–240.
[13] Y. Hanasaki, S. Ogawa, S. Fukui, The correlation between active oxygens scavenging and antioxidative effects of flavonoids, Free Radic. Biol. Med. 16 (1994) 845–850.
[14] X. Qin, X. Hou, M. Zhang, T. Liang, J. Zhi, L. Han, Q. Li, Relaxation of rat aorta by farrerol correlates with potency to reduce intracellular calcium of VSMCs, Int. J. Mol. Sci. 15 (2014) 6641–6656.
[15] Z. Liu, X. Zheng, Y. Wang, M. Tang, S. Chen, F. Zhang, L. Li, C. Zhang, Y. Sun, Lignans and isoflavonoids from the stems of *Pisonia umbellifera*, RSC Adv. 8 (2018) 16383–16391.
[16] L.J. Zhu, S. Yi, X. Li, H.F. Chen, M. Ming, X. Zhang, X.S. Yao, *C*-glycosides from the stems of *Calophyllum membranaceum*, J. Asian Nat. Prod. Res. 20 (2017) 1–6.
[17] J.B. Thoden, C.A. Sellick, D.J. Timson, R.J. Reece, H.M. Holden, Molecular structure of *Saccharomyces cerevisiae* Gal1p, a bifunctional galactokinase and transcriptional inducer, J. Biol. Chem. 280 (2005) 36905–36911.
[18] M. Bai, G.D. Yao, S.F. Liu, D. Wang, Q.B. Liu, X.X. Huang, S.J. Song, Lignans from a wild vegetable (*Patrinina villosa*) able to combat Alzheimer's disease, J. Funct. Foods 28 (2017) 106–113.
[19] T. Tanaka, T. Nakashima, T. Ueda, K. Tomii, I. Kouno, Facile discrimination of aldose enantiomers by reversed-phase HPLC, Chem. Pharm. Bull. 55 (2007) 899–901.
[20] Y. Hattori, K.H. Horikawa, H. Makabe, N. Hirai, M. Hirota, T. Kamo, A refined method for determining the absolute configuration of the 3-hydroxy-3-methylglutaryl group, Tetrahedron-Asymmetr. 18 (2007) 1183–1186.
[21] W. Gaffeld, Circular dichroism, optical rotatory dispersion and absolute configuration of flavanones, 3-hydroxyflavanones and their glycosides: Determination of aglycone chirality in flavanone glycosides, Tetrahedron 26 (1970) 4093–4108.
[22] P. Basnet, S. Kadota, M. Shimizu, H.X. Xu, T. Namba, 2′-Hydroxymatteucinol, a new *C*-methyl flavanone derivative from *Matteccia orientalis*; potent hypoglycemic activity in streptozotocin (STZ)-induced diabetic rat, Chem. Pharm. Bull. 41 (1993) 1790–1795.
[23] Y.Z. Tang, J.H. Ling, P. Zhang, X.R. Zhang, N. Zhang, W.L. Wang, J.Y. Li, N. Li, Potential therapeutic agents for circulatory diseases from *Bauhinia glauca* Benth.subsp. *pernervosa*, Bioorg. Med. Chem. Lett. 25 (2015) 3217–3220.
[24] W.S. Feng, X.W. Cao, X.K. Zheng, H.X. Kuang, A new flavanone from *Dryopteris sublaeta*, Acta Pharm. Sin. 40 (2005) 443–446.
[25] H. Wada, N. Tanaka, T. Murakami, T. Uchida, K. Kozawa, Y. Saiki, C.M. Chen, Chemical and chemotaxonomical studies of filices. LXXVI.: An unusual flavanone derivative from *Wagneriopteris japonica* LOEVE *et* LOEVE, Yakugaku Zasshi 108 (1988) 740–744.
[26] W.S. Feng, X.W. Cao, H.X. Kuang, X.K. Zheng, Isolation and structure identification of a new flavanone from *Dryopteris sublaeta*, Chin. J. Nat. Med. 3 (2005) 336–339.
[27] T. Iwashina, J. Kitajima, S. Matsumoto, Flavonoids in the species of *Cyrtomium* (*Dryopteridaceae*) and related genera, Biochem. Syst. Ecol. 34 (2006) 14–24.
[28] S. Matsuura, Ring closure of chalcones to flavanones in the presence of concentrated orthophosphoric acid. II. Ring closure of chalcones derived from phloroglucinol monomethyl ethers, Yakugaku Zasshi 77 (1957) 296–298.
[29] X.W. Lou, Q.H. Lin, G.Y. Zhang, W.Y. Liu, F. Feng, W. Qu, Identification and characterization of three new flavonoids from *Rhododendron dauricum*, Chin. J. Nat. Med. 13 (2015) 628–633.
[30] K. Stich, G. Forkmann, Studies on columnidin biosynthesis with flower extracts from Columnea hybrida, Zeitschrift fuer Naturforschung C, J. Biosci. 43 (1988) 311–314.
[31] M. Linuma, M. Mizuno, Natural occurrence and synthesis of 2′-oxygenated flavones, flavonols, flavanones and chalcones, Phytochemistry 28 (1989) 681–694.
[32] W. Hakamata, M. Kurihara, H. Okuda, T. Nishio, T. Oku, Design and screening strategies for α-glucosidase inhibitors based on enzymological information, Curr. Top. Med. Chem. 9 (2009) 3–12.
[33] H. Cao, X. Chen, Structures required of flavonoids for inhibiting digestive enzymes, Anti-Cancer Agent Me. 12 (2012) 929–939.